ADVANCED FUNCTIONAL MATERIALS
www.afm-journal.de

Bio-Orthogonally Crosslinked, Engineered Protein Hydrogels with Tunable Mechanics and Biochemistry for Cell Encapsulation

*Christopher M. Madl, Lily M. Katz, and Sarah C. Heilshorn**

Covalently-crosslinked hydrogels are commonly used as 3D matrices for cell culture and transplantation. However, the crosslinking chemistries used to prepare these gels generally cross-react with functional groups present on the cell surface, potentially leading to cytotoxicity and other undesired effects. Bio-orthogonal chemistries have been developed that do not react with biologically relevant functional groups, thereby preventing these undesirable side reactions. However, previously developed biomaterials using these chemistries still possess less than ideal properties for cell encapsulation, such as slow gelation kinetics and limited tuning of matrix mechanics and biochemistry. Here, engineered elastin-like proteins (ELPs) are developed that crosslink via strain-promoted azide-alkyne cycloaddition (SPAAC) or Staudinger ligation. The SPAAC-crosslinked materials form gels within seconds and complete gelation within minutes. These hydrogels support the encapsulation and phenotypic maintenance of human mesenchymal stem cells, human umbilical vein endothelial cells, and murine neural progenitor cells. SPAAC-ELP gels exhibit independent tuning of stiffness and cell adhesion, with significantly improved cell viability and spreading observed in materials containing a fibronectin-derived arginine-glycine-aspartic acid (RGD) domain. The crosslinking chemistry used permits further material functionalization, even in the presence of cells and serum. These hydrogels are anticipated to be useful in a wide range of applications, including therapeutic cell delivery and bioprinting.

1. Introduction

Hydrogels are an attractive class of materials to serve as biomimetic scaffolds for 3D cell encapsulation, tissue engineering, and drug delivery applications.[1,2] Because of their high water content, hydrogels are an ideal platform for encapsulating living cells for both in vitro models studying cell–matrix interactions, as well as for delivering cells for therapeutic applications and controlling the fate of the cells post-transplantation.[2] Many such applications use covalently-crosslinked chemical hydrogels due to their increased stability and improved mechanical properties relative to physical hydrogels.[3] One of the limitations of many chemical hydrogel systems currently used for cell encapsulation is nonspecific side reactions of the crosslinking chemistry with cells and other biological entities embedded within the gels. Covalently crosslinked hydrogels often make use of photoinitiators or catalysts that are potentially cytotoxic or rely on crosslinking chemistries that also react with biological moieties present on cells and co-delivered biological factors, such as amines and sulphydryls.[3] Significant progress over the past decades has been made in developing bio-orthogonal chemistries that do not cross-react with functional groups found in biology.[4] Such chemistries include copper(I)-catalyzed azide-alkyne cycloaddition (CuAAC),[5] Staudinger ligation,[6] strain-promoted azide-alkyne cycloaddition (SPAAC),[7] tetrazine ligation,[8] and traditional Diels–Alder reactions.[3]

The first hydrogels crosslinked using bio-orthogonal chemistries made use of CuAAC;[9] however, this crosslinking chemistry is not suitable for encapsulating living cells, due to the use of a cytotoxic copper catalyst.[7] More recently, catalyst-free bio-orthogonal crosslinking strategies have been developed for a wide range of hydrogel materials that eliminate the potential of cytotoxicity and permit cell encapsulation within the materials.[3,10] Both synthetic materials, such as poly(ethylene glycol) (PEG)[11–13] and naturally derived polymers, such as hyaluronic acid[14–16] and alginate,[17,18] have been functionalized to crosslink by Staudinger ligation,[18] SPAAC,[11] tetrazine ligation,[12,17,19] and Diels–Alder reactions.[13–16] While these previous systems have overcome the issue of copper cytotoxicity associated with CuAAC crosslinking, several limitations remain. The gelation kinetics of many bio-orthogonal chemistries are not conducive to cell encapsulation. For instance, Diels–Alder reactions between furan and maleimide moieties result in gelation times ranging from tens to hundreds of minutes,[13,15,16] which is too slow to achieve homogeneous cell dispersion within the gel and can result in decreased cell

C. M. Madl
Department of Bioengineering
Stanford University
Stanford, CA 94305, USA
L. M. Katz, Prof. S. C. Heilshorn
Department of Materials Science and Engineering
Stanford University
Stanford, CA 94305, USA
E-mail: heilshorn@stanford.edu

DOI: 10.1002/adfm.201505329

viability.[15] On the other hand, the reaction between tetrazines and *trans*-cyclooctenes proceeds too rapidly to achieve uniform gelation and cell encapsulation by simple mixing.[19] Synthetic polymers, such as PEG, are bio-inert and must be further functionalized to permit biological functions such as cell adhesion[20] and proteolytic degradation.[21] Naturally derived polymers can be subject to batch-to-batch variation,[22] and polysaccharides such as alginate and hyaluronic acid must still be modified to permit integrin-mediated cell adhesion[23] and proteolytic degradation.[24] Furthermore, hydrogels comprised of synthetic or naturally harvested polymers generally lack independent tuning of such critical material parameters as initial mechanical properties, cell adhesivity, and degradation.[25] The use of recombinant protein engineered materials provides the potential to overcome the inherent limitations of these existing material systems. As protein synthesis is a form of templated polymerization, recombinant protein-based materials do not suffer from batch-to-batch variation.[26] This templated polymerization also allows one to directly specify the biochemical properties of the material, eliminating the need for further functionalization with bioactive peptides to permit cell adhesion and proteolytic degradation.[26] Furthermore, modular design strategies have been employed to produce protein-based materials with decoupled matrix mechanics and biochemistry.[27]

Here we develop recombinant elastin-like proteins (ELPs) that crosslink via bio-orthogonal SPAAC reactions for use as cell-encapsulating hydrogels. These ELPs take advantage of modular protein design strategies that permit independent tuning of matrix mechanics and biochemistry: bioactive domains containing an extended arginine-glycine-aspartic acid (RGD) sequence derived from fibronectin alternate with elastin-like domains containing lysine residues used for chemical modification and subsequent crosslinking (**Figure 1**A). To facilitate crosslinking, the primary amines of these lysines are functionalized with either azide moieties or bicyclo[6.1.0]nonyne (BCN) groups. Upon mixing, ELPs with azide and BCN groups crosslink via SPAAC, forming a gel within seconds. These gels support the viability and phenotypic maintenance of encapsulated human mesenchymal stem cells (hMSCs), human umbilical vein endothelial cells (HUVECs), and murine neural progenitor

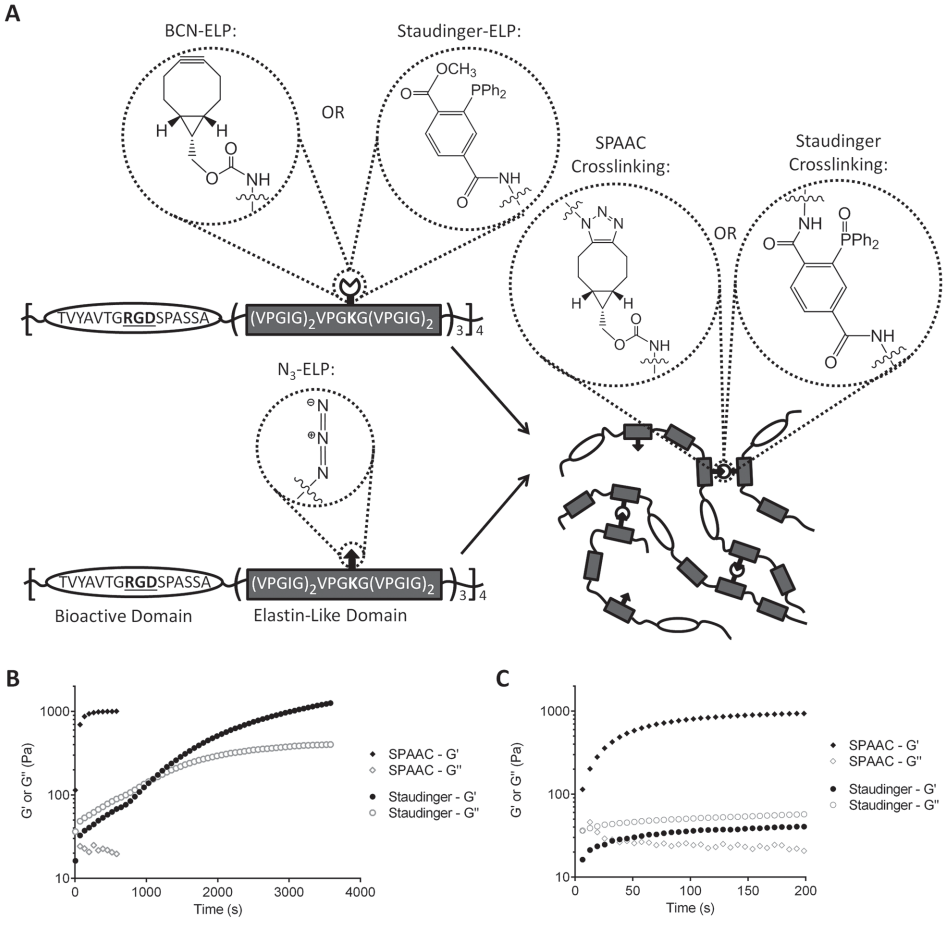

Figure 1. Crosslinking chemistry regulates gelation kinetics in bio-orthogonally crosslinked ELP hydrogels. A) To facilitate bio-orthogonal crosslinking, ELPs are functionalized with azides (N_3-ELP) and either strained cyclooctynes (BCN-ELP) or triarylphosphines (Staudinger-ELP). Upon mixing, the functionalized ELPs crosslink by either strain-promoted azide-alkyne cycloaddition (SPAAC) or Staudinger ligation to form hydrogels. Please note that the degree of BCN, triarylphosphine, and azide substitution can be varied, resulting in modification of less than all 12 lysine residues. Theoretical and measured degrees of substitution are listed in Table 1. B) Time sweep showing storage (G′) and loss (G″) moduli during bio-orthogonal ELP gelation. C) Time sweep data from 0 to 200 s illustrate rapid crosslinking of SPAAC-based gels.

Adv. Funct. Mater. **2016**,
DOI: 10.1002/adfm.201505329

cells (mNPCs) in vitro. SPAAC-ELP hydrogels exhibit independent tuning of storage modulus and cell-adhesive ligand presentation, with both viability and cell spreading in hMSCs regulated by RGD content. Furthermore, these gels present additional sites for bio-orthogonal functionalization post-cell encapsulation, adding the potential for further modification with bioactive factors at later times.

2. Results and Discussion

2.1. Bio-Orthogonal Crosslinking of ELP Hydrogels

ELPs containing either cell-adhesive, fibronectin-derived extended RGD sequences or nonadhesive, scrambled arginine-aspartic acid-glycine (RDG) sequences were produced by recombinant protein engineering techniques.[27] These ELPs were further functionalized with azides as well as either BCN or triarylphosphines to facilitate SPAAC or Staudinger ligation-mediated crosslinking, respectively (Figure 1A). The ELPs were designed to contain lysines within the elastin-like domain to permit further chemical modification. Azides were introduced at these lysines via an aqueous diazo transfer reaction to yield azide-ELP (N_3-ELP).[28] Diazo transfer using imidazole-1-sulfonyl azide, as opposed to the traditional approach using trifluoromethanesulfonyl azide, has several advantages, including decreased risk of explosion, enhanced shelf-life, and the ability to react successfully in protic solvents.[28,29] Azide functionalization was confirmed via Fourier transform infrared spectroscopy (FT-IR) (Figure S1, Supporting Information), and the degree of azide substitution per ELP polymer was estimated using ^{1}H-NMR (**Table 1**; Figure S2, Supporting Information). The lysine residues in the elastin-like domain also facilitated functionalization with activated esters of BCN and the triarylphosphine reagent to form BCN-ELP and Staudinger-ELP, respectively. BCN was chosen as the strained alkyne for SPAAC crosslinking because the synthesis of BCN is simpler and results in higher yield when compared with other cylcooctynes used in SPAAC reactions,[30] providing for easier scale-up in the future. Successful conjugation of BCN and the triarylphosphine to ELP was confirmed with ^{1}H-NMR (Figure S2, Supporting Information). Degree of substitution was also estimated from ^{1}H-NMR (Table 1).

The gelation kinetics of SPAAC- and Staudinger-crosslinked ELPs were observed using oscillatory rheology (Figure 1B). Upon mixing of N_3-ELP with BCN-ELP in aqueous solution (3:1 molar ratio of azide to BCN), SPAAC crosslinking induced the polymers to gel within seconds, as is evidenced by a greater storage modulus (G′) than loss modulus (G″) by the time the rheometer started to take measurements. All formulations of SPAAC-crosslinked materials completed gelation in a matter of minutes, reaching half their maximal storage modulus in less than 1 min (Table 1; Figure S3, Supporting Information). ELPs crosslinked by Staudinger ligation (i.e., mixing of N_3-ELP with Staudinger-ELP to result in a 3:1 molar ratio of azide to triaylphosphine) take significantly longer to gel, reaching their critical gelation point (G′ > G″) after ≈20 min (Table 1) and their plateau modulus on the order of 1 h (Figure 1B). Excess azide relative to BCN and triarylphospine was utilized to force the reaction rapidly to completion, as well as to permit further bio-orthogonal functionalization of the hydrogels post-gelation, as described below. Sufficient diazo transfer reagent was added to functionalize the 12 primary amines present in the elastin-like domains of the ELP, and the amount of BCN and triarylphosphine functionalization was varied to yield gels with biologically relevant stiffnesses (G′ ≈ 100s to 1000s of Pa).[31] Due to the hydrophobic nature of the BCN and triarylphosphine groups, the degree of substitution of these groups per ELP polymer was also carefully controlled to maintain the solubility of the proteins in physiological salt solutions.

The rapid gelation kinetics of SPAAC-crosslinked ELP gels would make them attractive materials for applications such as cell transplantation through injection and bioprinting. Similar to previous approaches delivering hydrogels crosslinked by hydrazone linkages,[32] the azide- and BCN-functionalized ELP components can be separately loaded into a dual barrel syringe and mixed during the injection or extrusion process. Rapid gelation for injected materials is desirable to increase material retention at the targeted injection site and to prevent undesired secondary effects, such as embolism resulting from partially gelled fragments that may enter the bloodstream.[33] Additionally, when printing complex 3D structures, rapid gelation is necessary to ensure high print fidelity and to limit the total time required to print the engineered tissue construct.[34] While rapid gelation is ideal for cell encapsulation, certain acellular applications may benefit from the slower gelation kinetics provided by the Staudinger ligation-based crosslinking, such as when using molds to cast gels in complicated 3D structures or when directly crosslinking drugs into implantable hydrogels.[35]

Table 1. Characterization of bio-orthogonal ELPs.

Functional group	Theoretical degree of substitution	Measured degree of substitution[a)]	Gelation time [s]
Azide	12	11	–
BCN	4	4.2	44 ± 1.5[b)]
	5	5.2	53 ± 1.6[b)]
Staudinger	4	4.4	1200 ± 120[c)]

[a)]Determined by ^{1}H-NMR; [b)]Time to half-maximal storage modulus for 5% (w/v) SPAAC gels, determined by fitting a first-order exponential association model; [c)]Time at which the storage modulus first exceeded the loss modulus for 5% (w/v) Staudinger gels.

2.2. Cell Encapsulation in Hydrogels with Tunable Mechanics

Because rapid gelation kinetics are ideal for cell encapsulation, SPAAC-crosslinked hydrogels were used for subsequent studies. The mechanical properties of the hydrogels can be tuned either by varying the molar ratio of BCN groups per ELP polymer or the polymer content of the hydrogel (**Figure 2**A,B; Figure S4, Supporting Information). SPAAC-crosslinked ELP gels were found to exhibit a linear viscoelastic response and behave as predominantly elastic materials (G′ > G″) in the range of oscillatory frequencies between 0.1 and 10 Hz (Figure 2A,B). As expected for elastic materials, increasing the crosslinking density by changing the molar ratio of BCN:ELP from 4:1 to 5:1

at a fixed polymer content of 5% (w/v) results in an increase in storage modulus from ≈1200 to ≈3300 Pa. Further varying the BCN:ELP ratio by blending 4:1 BCN-functionalized ELP with 5:1 BCN-functionalized ELP in 1:1 ratio to achieve a BCN:ELP ratio of 4.5:1 resulted in gels with an intermediate modulus of ≈2300 Pa (Figure S3B, Supporting Information). At a fixed BCN:ELP ratio of 4:1, varying the polymer content of the gels from 2% to 3% to 5% (w/v) results in storage moduli of ≈180, ≈360, and ≈1200 Pa, respectively.

To demonstrate the cytocompatibility of the SPAAC-based crosslinking procedure, hMSCs, HUVECs, or mNPCs were encapsulated in SPAAC-ELP hydrogels with storage moduli of ≈1200 Pa (hMSCs) or ≈360 Pa (HUVECs and mNPCs). To confirm that the bio-orthogonal SPAAC crossslinking reaction was not cytotoxic, acute viability following crosslinking was assessed using a Live/Dead cytotoxicity assay. One-hour post-encapsulation, all three cell types remained highly viable, with live cell fractions of 99% ± 0.52% for hMSCs, 97% ± 1.0% for HUVECs, and 97% ± 0.37% for mNPCs (Figure 2C,D). To determine if SPAAC-ELP hydrogels permitted phenotypic maintenance of these cell populations in vitro, cells encapsulated in RGD-containing, SPAAC-crosslinked gels were cultured for an additional 2–14 d. After 2 d, hMSCs exhibited a characteristic spread morphology with actin stress fibers,[36] as observed by phalloidin staining (Figure 2E). This cytoskeletal rearrangement into actin stress fibers is characteristic of hMSCs within 3D cultures that enable both cell adhesion to, and cell remodeling of, the matrix.[24,37] After one week in culture, HUVECs maintained expression of the endothelial marker CD31 and had begun to associate into tubular networks with open lumen-like structures, as observed by confocal microscopy of immunostained samples (Figure 2F). Both CD31 expression and tubulogenesis are hallmarks of endothelial cell phenotypic maintenance in vitro.[38] Murine NPCs cultured for one week within SPAAC-crosslinked ELP gels stained positive for the neural progenitor marker nestin (Figure 2G). Furthermore, mNPCs maintained the capacity to differentiate into neurons and astrocytes following an additional week of treatment with mixed differentiation medium, as evidenced by staining for the neuronal marker microtubule associated protein 2 (MAP2) and the astrocytic marker glial fibrillary acid protein (GFAP) (Figure 2H). Nestin expression and the ability to differentiate into neurons and glia

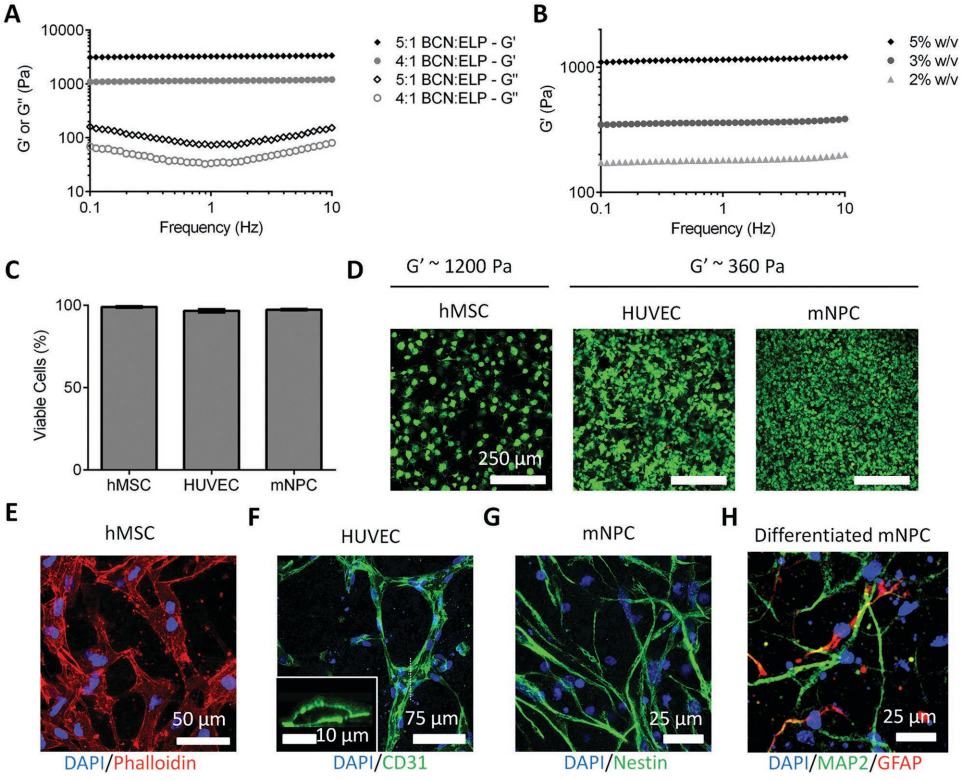

Figure 2. SPAAC-crosslinked ELP hydrogels exhibit tunable mechanics and maintain cell viability and phenotype in vitro. A) Average storage (G′) and loss (G″) moduli of SPAAC-crosslinked ELP gels during a frequency sweep at a fixed strain of 1%, varying the stoichiometry of BCN groups per ELP polymer at 5% (w/v) polymer content. B) Average storage moduli (G′) during a frequency sweep at a fixed strain of 1%, varying the polymer content of the hydrogels with a fixed BCN:ELP ratio of 4:1. C) Acute viability of hMSCs, HUVECs, and mNPCs 1 h post-encapsulation in SPAAC-crosslinked ELP hydrogels, quantified from Live/Dead imaging. Error bars are ± SD. D) Representative Live/Dead images demonstrating high acute cell viability in SPAAC-crosslinked ELP gels with different storage moduli. E) Human MSCs encapsulated in SPAAC-based gels exhibit a normal, spread phenotype with actin stress fibers after 2 d in culture. F) HUVECs in SPAAC-based ELP gels stain positive for the endothelial marker CD31 and self-organize into tubular networks after 7 d in culture. Inset: Orthogonal view showing open lumen-like structure in region denoted by dashed white line. G) Murine NPCs encapsulated in SPAAC-ELP gels stain positive for the neural progenitor marker nestin after 7 d in culture. H) NPCs maintain their differentiation capacity in SPAAC-crosslinked ELP gels, staining positive for the neuronal marker MAP2 and the astrocytic marker GFAP after 14 d of differentiation.

Adv. Funct. Mater. 2016,
DOI: 10.1002/adfm.201505329

are both indicative of an NPC phenotype.[39] These results indicate that SPAAC-crosslinked ELP hydrogels support the in vitro culture of the three cells types tested.

2.3. Independent Tuning of Matrix Mechanics and Biochemistry

The modular design of ELPs is a distinct advantage over other engineered materials used for cell encapsulation, in that this modularity allows for independent tuning of matrix mechanics and biochemistry.[27] To demonstrate that SPAAC-crosslinked ELPs retain the ability to decouple mechanics from biochemistry, cell-adhesive RGD-ELP and non-cell-adhesive RDG-ELP (**Figure 3**A) were modified with varying molar ratios of BCN:ELP. Increasing the BCN:ELP ratio from 4:1 to 5:1 resulted in a significant increase in storage modulus for both RGD- and RDG-ELP hydrogels (≈1400 to ≈3900 Pa for RGD-ELP gels and ≈1200 to ≈3300 Pa for RDG-ELP gels), whereas there was no significant difference in storage modulus between RGD- and RDG-ELP gels with the same degree of BCN substitution (Figure 3B). To demonstrate that the encoded matrix biochemistry can dictate cellular behavior, hMSCs were encapsulated in SPAAC-crosslinked gels containing varying concentrations of the cell-adhesive RGD ligand (0, 0.53, and 5.3mM). Furthermore, to illustrate the importance of decoupling matrix mechanics from biochemistry, the stiffness of the hydrogels was also varied from G′ ≈ 1200 to 3300 Pa. Cell viability within RGD-containing gels was significantly higher (up to 96%) than in nonadhesive RDG gels (72%–85%), as assessed by Live/Dead staining (Figure 3C,D; Figure S5A, Supporting Information). This agrees with previous studies showing decreased MSC viability with decreasing concentrations of adhesive ligand.[40] Human MSCs encapsulated within 5.3 mM RGD gels exhibited significantly increased cell spreading when compared to 0 M gels at both stiffnesses, as measured from maximum intensity projections of confocal micrographs of phalloidin-stained samples (Figure 3E,F; Figure S5B, Supporting Information). MSCs cultured in 5.3 mM RGD gels displayed a well-spread morphology with distinct actin stress fibers, indicative of strong cell–matrix adhesion, whereas MSCs cultured in non-adhesive gels appeared rounded without any noticeable stress fibers. At the intermediate RGD concentration, cell spreading was clearly dependent on the stiffness of the hydrogels. At 0.53 mM RGD, MSCs cultured in the 1200 Pa gels exhibited a well-spread

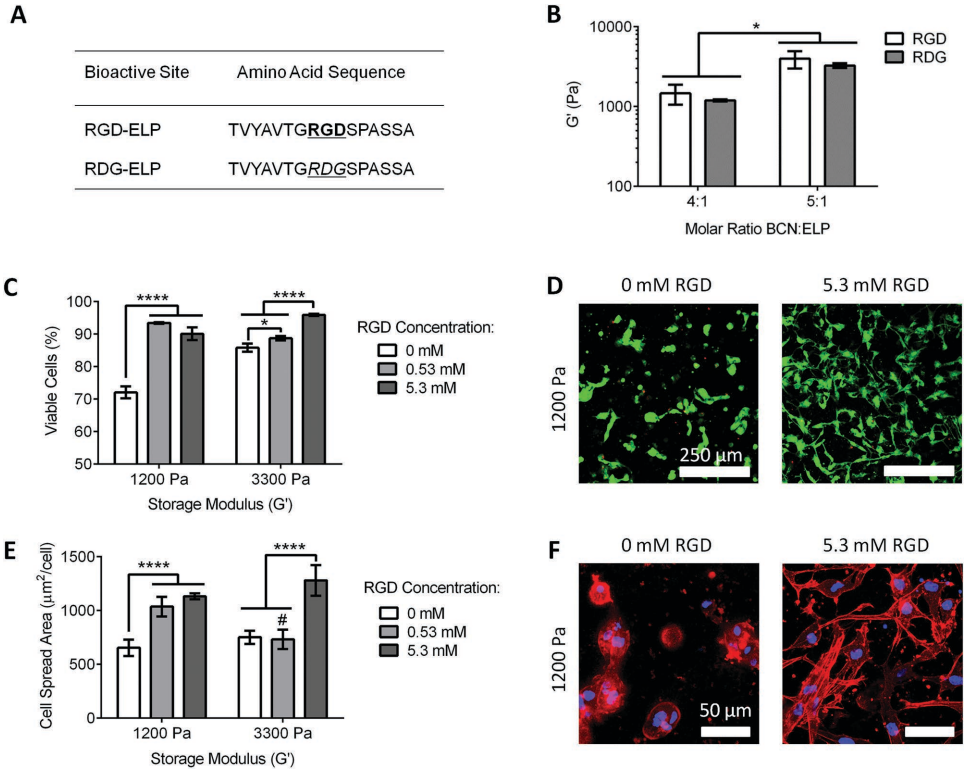

Figure 3. SPAAC-crosslinked ELP hydrogels exhibit decoupled control of matrix mechanics and biochemistry. A) The modular nature of ELPs allows facile tuning of cell adhesivity by producing variants with an extended RGD sequence derived from fibronectin or with a non-adhesive, scrambled RDG sequence. B) Storage moduli (G′) of RGD- and RDG-ELP gels at 1 Hz and 1% strain, demonstrating independent tuning of matrix mechanics and biochemistry. C) Viability of human MSCs cultured in SPAAC-ELP hydrogels with varying RGD concentration and stiffness after 2 d, quantified from Live/Dead staining. At a given RGD concentration, viability in 1200 Pa gels is significantly different from the viability in 3300 Pa gels at the same RGD concentration ($p < 0.001$). D) Representative Live/Dead staining for hMSCs encapsulated in hydrogels with RGD concentrations of 0 M (100% RDG-ELP) or 5.3 mM (100% RGD-ELP) after 2 d. Green: live (calcein-AM), red: dead (ethidium homodimer). E) Cell spread area for human MSCs cultured in SPAAC-ELP hydrogels with varying RGD concentration and stiffness after 2 d, quantified from phalloidin staining. #$p < 0.001$ relative to 1200 Pa, 0.53 mM condition. F) Representative staining demonstrating increased cell spreading in RGD-containing hydrogels after 2 d. Blue: nuclei (DAPI); red: F-actin (phalloidin). Error bars are ± SD. *$p < 0.05$, ****$p < 0.0001$.

morphology, similar to cells cultured in the 5.3 mM gels (Figure 3E; Figure S5B, Supporting Information). However, in the 3300 Pa gels, the MSCs were more rounded, with decreased spreading, appearing similar to cells in the 0 M gels. Previous studies have shown decreasing RGD ligand bond formation as hydrogel stiffness increases beyond a certain threshold, likely due to an inability of the MSCs to cluster the ligands and form stable adhesions in gels that are too stiff.[41] In that study, RGD ligand bond formation in the stiffer gels was rescued by increasing the concentration of RGD present in the gels, such that the local concentration seen by the cells would be sufficient to form adhesions without additional ligand clustering. This may account for the decreased cell spreading observed in the present study in stiffer ELP gels at an intermediate RGD density. RGD ligand concentration and hydrogel stiffness act synergistically in determining MSC viability and spreading in SPAAC-crosslinked ELP gels, as evidenced by significant interaction parameters in two-way analysis of variance (ANOVA) ($p < 0.001$). Taken together, these results indicate that SPAAC-crosslinked gels retain the bioactivity designed into the original ELP amino acid sequence, and that the matrix mechanics can be tuned independently of the encoded biochemistry. The independent tuning of matrix properties is critical, as both hydrogel stiffness and adhesive ligand concentration modulate cellular behavior in an interconnected manner.

2.4. Bio-Orthogonal Functionalization of Hydrogels

The bio-orthogonality of the SPAAC reaction can permit further functionalization of the hydrogels after cell encapsulation, even in the presence of biological entities, such as cells and serum. This bio-orthogonal feature of the SPAAC reaction was clearly demonstrated by Bertozzi and co-workers, who used SPAAC probes to image cell membrane-associated glycans in developing zebrafish.[42] To demonstrate bio-orthogonality within a hydrogel context, SPAAC-crosslinked ELP hydrogels were prepared using an excess of azides relative to BCN groups. Therefore, post-crosslinking, a large number of azides were still available for further reactions. To demonstrate that these excess azides permit additional, bio-orthogonal functionalization of the ELP gels, hMSCs were encapsulated in the SPAAC-crosslinked gels and cultured for 2 d. These samples were then treated with either a BCN-bearing fluorescent dye (CF640R BCN) or an unreactive control dye (CF640R amine) in serum-containing culture medium for 1 h (**Figure 4**A). The gels were subsequently washed to remove any unbound dye. Dye conjugation was quantified by degrading the gels with trypsin and measuring fluorescence intensity. The concentration of dye initially bound to the degraded hydrogels was estimated from a standard curve relating fluorescence intensity to soluble dye concentration. SPAAC-crosslinked gels treated with the BCN-modified dye exhibited significant fluorescence, indicating successful SPAAC reaction post-cell-encapsulation and culture (Figure 4B). Furthermore, the fluorescence observed in the control dye-treated samples was not significantly higher than the untreated samples, confirming that the increased fluorescence in the BCN dye-treated condition is due to specific reaction of the dye with the azides in the gels, and not due to nonspecific binding of dye to the ELP. Specific functionalization of the SPAAC-ELP gels with the BCN-bearing dye in the presence of cells was also confirmed by confocal microscopy (Figure 4C).

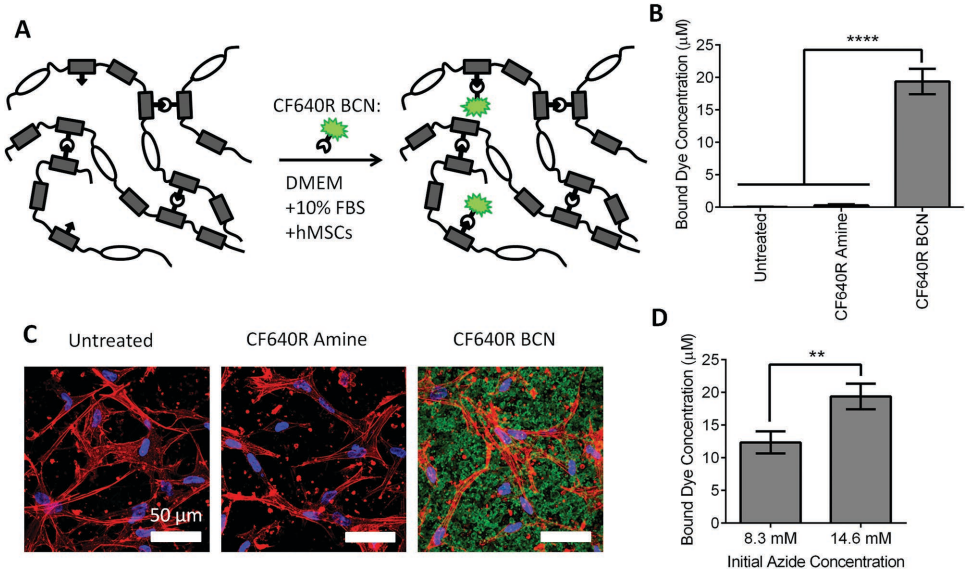

Figure 4. Bio-orthogonal functionalization of cell-laden SPAAC-crosslinked ELP hydrogels. A) Excess azide groups on the SPAAC-crosslinked gels permit further functionalization of the gels with a BCN-containing fluorescent probe. As the reaction between BCN and azide is bio-orthogonal, the reaction can occur in the presence of cells and serum. B) Concentration of bound fluorescent dye conjugated to hMSC-containing gels that were untreated or treated with either an unreactive control dye (CF640R Amine) or a reactive BCN-modified dye (CF640R BCN). C) Representative images demonstrating bio-orthogonal functionalization of SPAAC-crosslinked gels containing hMSCs. Bio-orthogonal dye conjugation was performed after 2 d in culture and in serum-containing culture medium. Blue: nuclei (DAPI), red: F-actin (phalloidin), green: fluorescent probe (CF640R). D) Concentration of bound fluorescent CF640R BCN dye conjugated to hMSC-containing gels with varying initial azide concentrations. Error bars are ± SD. $^{**}p < 0.01$, $^{****}p < 0.0001$.

DOI: 10.1002/adfm.201505329

To further demonstrate the specificity and tunability of this bio-orthogonal functionalization, SPAAC-crosslinked ELP hydrogels were prepared using proteins presenting different initial concentrations of azide. Incorporation of the BCN-bearing fluorescent dye into these hMSC-containing gels in the presence of serum was measured as above. Consistent with the specific reaction between the BCN and azide groups, gels with lower initial azide concentration exhibited decreased dye incorporation relative to gels with higher azide concentration (12.4 μM vs 19.4 μM bound dye concentration, respectively) (Figure 4D). The ability to further functionalize the hydrogels can permit incorporation of additional cues to direct the phenotype of the encapsulated cells, such as bioactive growth factor mimetic peptides.[43,44] Delivering the dye as a 10 μM solution resulted in an accumulation of the dye within the hydrogels over the course of 1 h, with average bound dye concentrations reaching 19.4 μM. These concentrations are in a relevant regime for many bioactive factors, including growth factor mimicking peptides, which have previously shown efficacy bound to hydrogels at concentrations ranging from tens of nanomolar[44] to hundreds of micromolar.[43] Future optimization studies will be required for each specific bioactive molecule to explore the exact concentration range required to elicit the desired biofunctionality using this post-encapsulation modification technique. As this bio-orthogonal functionalization can occur post-encapsulation, it may allow for timed delivery of multiple biochemical factors, which is known to be important in the process of tissue development and has been previously employed in biomaterial systems to promote angiogenesis[45] and adipogenesis.[46] The concentration of azides remaining in the hydrogels post-gelation is ≈9 mM, meaning that a large excess of binding sites remain for the incorporation of additional factors. Recent studies have shown specific targeting using SPAAC-conjugation of fluorescent probes to hydrogels in a mouse model,[47] suggesting that bio-orthogonal functionalization of SPAAC-crosslinked ELP gels could be used in the future to localize factors to encapsulated cells post-implantation in vivo at desired times.

3. Conclusion

Engineered elastin-like protein hydrogels were prepared that crosslink via bio-orthogonal SPAAC and Staudinger ligation reactions. While Staudinger-crosslinked ELPs gelled too slowly for cell encapsulation, SPAAC-crosslinked ELPs gelled within seconds and reached their plateau storage moduli within a few minutes. These SPAAC-ELP gels supported the in vitro culture of hMSCs, HUVECs, and mNPCs with >97% acute viability and longer term phenotypic maintenance for all cell types tested. SPAAC-crosslinked gels exhibited independent tuning of matrix elasticity and cell-adhesive ligand presentation by varying the crosslinking stoichiometry and the amino acid sequence of the bioactive protein domains, respectively. Gels containing the cell-adhesive extended RGD sequence derived from fibronectin supported enhanced viability and spreading of hMSCs compared to gels containing a non-adhesive, scrambled RDG sequence. Furthermore, the same bio-orthogonal chemistry employed to crosslink the gels can be exploited post-cellencapsulation to specifically add new functionality to the gels, even in the presence of cells and serum. These features make SPAAC-crosslinked ELP hydrogels attractive materials for applications such as therapeutic cell injection and bioprinting.

4. Experimental Section

Materials: Reagents were purchased from either Sigma-Aldrich or Fisher and used without further purification unless otherwise noted.

Preparation of Elastin-Like Proteins: ELPs containing either cell-adhesive RGD domains derived from human fibronectin or non-adhesive scrambled RDG domains were produced separately using recombinant protein engineering techniques, as previously described.[27] Briefly, pET15b plasmids encoding the ELPs under control of the T7 promoter were transformed into BL21(DE3)pLysS *Escherichia coli* (Life Technologies). The bacteria were grown in Terrific Broth to an optical density of 0.8, at which point ELP expression was induced by the addition of isopropyl *β*-D-1-thiogalactopyranoside to a final concentration of 1 mM. After 7 h, the bacteria were pelleted, resuspended in TEN buffer (100 mM sodium chloride, 10 mM Tris, 1 mM ethylenediaminetetraacetic acid (EDTA) at pH 8.0), and lysed via repetitive freeze/thaw in the presence of 1 mM phenylmethylsulfonyl fluoride protease inhibitor. Taking advantage of the lower critical solution temperature behavior of ELP, the ELPs were purified by subjecting the cell lysates to repetitive temperature cycling: ELP was dissolved into deionized water at 4 °C and adjusted to pH 9.0, and ELP precipitation at 37 °C was aided by the addition of 1 M sodium chloride. Purified ELP was desalted by dialyzing against deionized water and then lyophilized to afford the protein as a white powder. Protein purity was confirmed via sodium dodecyl sulfate-polyacrylamide gel electrophoresis.

Synthesis and Characterization of Functionalized ELPs: Azide functional groups were introduced into ELP via aqueous diazo transfer.[28] ELP was dissolved to a final concentration of 2.5% (w/v) in freshly prepared potassium carbonate buffer (10 mg mL^{-1} in deionized water). One hundred microliters of a copper(II) chloride solution (1 mg mL^{-1}) was added per milliliter of ELP solution, followed by the addition of sufficient 1H-imidazole-1-sulfonyl azide HCl, dissolved in potassium carbonate buffer, to result in a theoretical degree of substitution of 12 azides per ELP molecule. The mixture was allowed to react for 24 h at room temperature with constant agitation. The azide-functionalized ELP was purified by dialyzing against distilled water and lyophilized to afford the product as a white powder. Azide incorporation was confirmed by FT-IR, and the degree of azide substitution was estimated from ^{1}H-NMR.

In order to functionalize ELP with BCN for SPAAC and triarylphosphines for Staudinger ligation, ELP was dissolved in anhydrous dimethyl sulfoxide (DMSO) to a final concentration of 2% (w/v). Four to five molar equivalents of either (1*R*,8*S*,9*S*)-bicyclo[6.1.0]-non-4-yn-9-ylmethyl *N*-succinimidyl carbonate (BCN-NHS; for SPAAC) or 2-(diphenylphosphino)terephthalic acid 1-methyl 4-pentafluorophenyl diester (for Staudinger ligation) were added to the ELP solution while stirring. Triethylamine (1.5 eq) was then added as a basic catalyst. The reaction was allowed to proceed for 24 h at room temperature with constant stirring. The BCN- and triarylphosphine-functionalized ELP was purified by dialyzing against distilled water and lyophilized to afford the product as a white powder. Successful conjugation and estimated degree of substitution for BCN and triarylphosphine modified ELPs were determined using ^{1}H-NMR.

Rheological Characterization of Bio-Orthogonal ELP Hydrogels: Solutions of azide-, BCN-, and triarylphosphine-modified ELPs were prepared by dissolving ELPs to 5% (w/v) in phosphate-buffered saline (PBS) at 4 °C. To determine gelation time, either BCN- or triarylphosphine-ELP was mixed in a 1:1 volumetric ratio with azide-ELP, and time sweeps were performed at room temperature (25 °C) on an ARG2 rheometer at 1% strain and 1 Hz oscillatory frequency. These parameters were determined to be within the linear viscoelastic regime (Figure 2A,B;

Figure S4A,B, Supporting Information). For Staudinger-crosslinked ELP, the gelation time was determined as the point at which the storage modulus (G′) first exceeded the loss modulus (G″). SPAAC-crosslinked ELP gels crossed this gelation threshold within seconds, prior to the start of measurements by the rheometer. Therefore, to estimate the timescale for SPAAC-based gelation, a first order exponential association model was fit to the SPAAC time sweep data and used to calculate the time at which the gels reached half of their maximum storage modulus. For mechanical characterization, the hydrogels were allowed to crosslink in situ on the rheometer. The gels were incubated for 10 min at 25 °C before the temperature was increased to 37 °C. After 5 min of equilibration at 37 °C, frequency sweeps from 0.1–10 Hz with a fixed 1% strain, and strain sweeps from 0.1% to 100% strain with a fixed 1 Hz oscillatory frequency, were performed. A solvent trap was used during all rheological measurements to prevent sample dehydration.

Cell Culture and Analysis: hMSCs were purchased from Lonza and expanded in Dulbecco's modified Eagle medium (DMEM) plus 10% fetal bovine serum (FBS), GlutaMAX, penicillin/streptomycin, and nonessential amino acids (Life Technologies). HUVECs were purchased from Lonza and expanded in EGM-2 (Lonza). mNPCs, isolated from subdissected dentate gyrus,[48] were a kind gift from Prof. Theo Palmer (Stanford Medical School). Murine NPCs were expanded in Neurobasal A medium supplemented with 2% B27, GlutaMAX (Life Technologies), 20 ng mL^{-1} FGF-2, and 20 ng mL^{-1} EGF (PeproTech) on polyornithine- and laminin-coated tissue culture plastic. Prior to encapsulation in bio-orthogonally crosslinked ELP hydrogels, cells were lifted via trypsinization, counted, and pelleted by centrifugation. Cell pellets were resuspended in either a 5% (w/v) azide-ELP solution (hMSCs) or a 3% (w/v) azide-ELP solution (HUVECs and mNPCs) in PBS at twice the desired final cell density (final densities: 2×10^6 cells mL^{-1} for hMSCs, 1×10^7 cells mL^{-1} for HUVECs, and 5×10^7 cells mL^{-1} for mNPCs). An equal volume of BCN-ELP at either 5% (w/v) (hMSCs) or 3% (w/v) (HUVECs and mNPCs) in PBS was then added. The cell suspensions were mixed thoroughly, and the gels were cast in 4 mm diameter × 0.5 mm deep silicone molds. The gels were allowed to crosslink for 10 min at room temperature and then were covered with the appropriate expansion medium. For hMSC studies, hydrogels were prepared to contain 0–5.3 mM RGD by blending adhesive RGD-ELP with non-adhesive RDG-ELP. HUVECs and mNPCs were cultured in hydrogels made entirely of RGD-ELP, which resulted in an RGD concentration of 3.2 mM within the 3% (w/v) gels. HUVEC and mNPC media were replenished every other day. For NPC differentiation, encapsulated mNPCs were maintained in expansion medium for 1 week before being treated with mixed differentiation medium (Neurobasal A plus 2% B27, GlutaMAX, 1% FBS, and 1 μM retinoic acid)[49] for an additional week. Cell viability was assessed via Live/Dead staining (Life Technologies), following the manufacturer's instructions. For immunofluorescence imaging, samples were fixed with 4% paraformaldehyde, permeabilized with 0.25% (v/v) Triton X-100 in PBS, and blocked with 5% (w/v) BSA and 5% (v/v) goat serum in PBS. Samples were then treated with primary antibodies as appropriate: mouse anti-CD31 (1:100, Cell Signaling), mouse anti-nestin (1:400, BD Pharmingen), rabbit anti-MAP2 (1:400, Millipore), and chicken anti-GFAP (1:300, Aves Labs). The samples were washed and then stained with the appropriate secondary antibodies: goat anti-mouse AF488 (1:500, Life Technologies), goat anti-rabbit AF546 (1:500, Life Technologies), and goat anti-chicken AF647 (1:400, Abcam). 4′,6-diamidino-2-phenylindole (DAPI) was included as a nuclear counterstain. Samples were imaged using a Leica SPE confocal microscope. Images were presented as maximum intensity projections of collected z-stacks and were analyzed using ImageJ software (NIH).

Functionalization of Cell-Encapsulating Hydrogels with Bio-Orthogonal Fluorescent Probe: Human MSCs were encapsulated in SPAAC-crosslinked ELP gels as described above. The cells were cultured for 2 d in hMSC expansion medium, at which point the samples were treated with complete expansion medium containing the fluorescent CF640R BCN dye or an unreactive control CF640R amine dye (10 μM, Biotium) for 1 h at 37 °C. After dye treatment, the samples were washed with PBS and either digested with 0.5% Trypsin/EDTA (Life Technologies) or fixed with 4% paraformaldehyde. Fluorescent intensity of digested samples was measured using a Molecular Devices SpectraMax M2 plate reader. Fixed samples were permeabilized with 0.25% (v/v) Triton X-100 in PBS, stained with DAPI and TRITC-Phalloidin, and imaged as above.

Statistical Analysis: Two-tailed Student's *t*-tests were used when comparing two experimental groups, and one-way ANOVA with Bonferroni post hoc testing was used to compare more than two experimental groups. The interaction between RGD ligand concentration and hydrogel stiffness on MSC viability and spreading was assessed using two-way ANOVA.

Supporting Information

Supporting Information is available from the Wiley Online Library or from the author.

Acknowledgements

The authors would like to thank Dr. Abbygail Foster and Dr. Lei Cai for assistance with NMR, and Prof. Theo Palmer and Dr. Harish Babu for providing the murine NPCs. C.M.M. acknowledges support from an NIH NRSA predoctoral fellowship (1 F31 EB020502-01). Development of the bio-orthogonal crosslinking chemistry and NMR characterization were supported by the Department of Energy, Office of Basic Energy Sciences, Materials Sciences and Engineering Division, under contract DE-AC02-76SF00515. Hydrogel characterization and in vitro cell culture were supported by the National Institutes of Health (1 U19 AI116484-01 and 5 R21 EB018407-02), National Science Foundation (DMR 1508006), and California Institute for Regenerative Medicine (RT3-07948).

Received: December 10, 2015
Revised: February 5, 2016
Published online:

[1] K. Y. Lee, D. J. Mooney, *Chem. Rev.* **2001**, *101*, 1869.
[2] a) D. J. Mooney, H. Vandenburgh, *Cell Stem Cell* **2008**, *2*, 205; b) B. D. Ratner, S. J. Bryant, *Annu. Rev. Biomed. Eng.* **2004**, *6*, 41.
[3] Y. Jiang, J. Chen, C. Deng, E. J. Suuronen, Z. Zhong, *Biomaterials* **2014**, *35*, 4969.
[4] a) J. A. Prescher, C. R. Bertozzi, *Nat. Chem. Biol.* **2005**, *1*, 13; b) E. M. Sletten, C. R. Bertozzi, *Angew. Chem. Int. Ed.* **2009**, *48*, 6974.
[5] a) V. V. Rostovtsev, L. G. Green, V. V. Fokin, K. B. Sharpless, *Angew. Chem. Int. Ed.* **2002**, *41*, 2596; b) C. W. Tornøe, C. Christensen, M. Meldal, *J. Org. Chem.* **2002**, *67*, 3057.
[6] E. Saxon, C. R. Bertozzi, *Science* **2000**, *287*, 2007.
[7] J. M. Baskin, J. A. Prescher, S. T. Laughlin, N. J. Agard, P. V. Chang, I. A. Miller, A. Lo, J. A. Codelli, C. R. Bertozzi, *Proc. Natl. Acad. Sci. USA* **2007**, *104*, 16793.
[8] N. K. Devaraj, R. Weissleder, S. A. Hilderbrand, *Bioconjugate Chem.* **2008**, *19*, 2297.
[9] a) D. A. Ossipov, J. Hilborn, *Macromolecules* **2006**, *39*, 1709; b) M. Malkoch, R. Vestberg, N. Gupta, L. Mespouille, P. Dubois, A. F. Mason, J. L. Hedrick, Q. Liao, C. W. Frank, K. Kingsbury, C. J. Hawker, *Chem. Commun.* **2006**, *14*, 2774.
[10] C. M. Nimmo, M. S. Shoichet, *Bioconjugate Chem.* **2011**, *22*, 2199.
[11] a) C. A. DeForest, B. D. Polizzotti, K. S. Anseth, *Nat. Mater.* **2009**, *8*, 659; b) C. D. Hermann, D. S. Wilson, K. A. Lawrence, X. Ning, R. Olivares-Navarrete, J. K. Williams, R. E. Guldberg, N. Murthy, Z. Schwartz, B. D. Boyan, *Biomaterials* **2014**, *35*, 9698.
[12] D. L. Alge, M. A. Azagarsamy, D. F. Donohue, K. S. Anseth, *Biomacromolecules* **2013**, *14*, 949.

[13] S. Kirchhof, F. P. Brandl, N. Hammer, A. M. Goepferich, *J. Mater. Chem. B* **2013**, *1*, 4855.
[14] C. M. Nimmo, S. C. Owen, M. S. Shoichet, *Biomacromolecules* **2011**, *12*, 824.
[15] F. Yu, X. Cao, Y. Li, L. Zeng, J. Zhu, G. Wang, X. Chen, *Polym. Chem.* **2014**, *5*, 5116.
[16] M. Fan, Y. Ma, Z. Zhang, J. Mao, H. Tan, X. Hu, *Mater. Sci. Eng. C* **2015**, *56*, 311.
[17] R. M. Desai, S. T. Koshy, S. A. Hilderbrand, D. J. Mooney, N. S. Joshi, *Biomaterials* **2015**, *50*, 30.
[18] K. M. Gattas-Asfura, C. L. Stabler, *Biomacromolecules* **2009**, *10*, 3122.
[19] H. Zhang, K. T. Dicker, X. Xu, X. Jia, J. M. Fox, *ACS Macro Lett.* **2014**, *3*, 727.
[20] a) F. Yang, C. G. Williams, D.-a. Wang, H. Lee, P. N. Manson, J. Elisseeff, *Biomaterials* **2005**, *26*, 5991; b) J. A. Burdick, K. S. Anseth, *Biomaterials* **2002**, *23*, 4315.
[21] a) M. P. Lutolf, G. P. Raeber, A. H. Zisch, N. Tirelli, J. A. Hubbell, *Adv. Mater.* **2003**, *15*, 888; b) S. Kim, E. H. Chung, M. Gilbert, K. E. Healy, *J. Biomed. Mater. Res., Part A* **2005**, *75A*, 73.
[22] a) Y. Li, J. Rodrigues, H. Tomás, *Chem. Soc. Rev.* **2012**, *41*, 2193; b) P. M. Kharkar, K. L. Kiick, A. M. Kloxin, *Chem. Soc. Rev.* **2013**, *42*, 7335.
[23] J. A. Rowley, G. Madlambayan, D. J. Mooney, *Biomaterials* **1999**, *20*, 45.
[24] S. Khetan, M. Guvendiren, W. R. Legant, D. M. Cohen, C. S. Chen, J. A. Burdick, *Nat. Mater.* **2013**, *12*, 458.
[25] a) L. Little, K. E. Healy, D. Schaffer, *Chem. Rev.* **2008**, *108*, 1787; b) M. E. Davis, P. C. H. Hsieh, A. J. Grodzinsky, R. T. Lee, *Circ. Res.* **2005**, *97*, 8.
[26] N. H. Romano, D. Sengupta, C. Chung, S. C. Heilshorn, *Biochim. Biophys. Acta* **2011**, *1810*, 339.
[27] K. S. Straley, S. C. Heilshorn, *Soft Matter* **2009**, *5*, 114.
[28] S. F. M. van Dongen, R. L. M. Teeuwen, M. Nallani, S. S. van Berkel, J. J. L. M. Cornelissen, R. J. M. Nolte, J. C. M. van Hest, *Bioconjugate Chem.* **2009**, *20*, 20.
[29] E. D. Goddard-Borger, R. V. Stick, *Org. Lett.* **2007**, *9*, 3797.
[30] J. Dommerholt, S. Schmidt, R. Temming, L. J. A. Hendriks, F. P. J. T. Rutjes, J. C. M. van Hest, D. J. Lefeber, P. Friedl, F. L. van Delft, *Angew. Chem. Int. Ed.* **2010**, *49*, 9422.
[31] A. J. Engler, S. Sen, H. L. Sweeney, D. E. Discher, *Cell* **2006**, *126*, 677.
[32] B. P. Purcell, D. Lobb, M. B. Charati, S. M. Dorsey, R. J. Wade, K. N. Zellars, H. Doviak, S. Pettaway, C. B. Logdon, J. A. Shuman, P. D. Freels, J. H. Gorman III, R. C. Gorman, F. G. Spinale, J. A. Burdick, *Nat. Mater.* **2014**, *13*, 653.
[33] R. McLemore, in *Injectable Biomaterials: Science and Applications* (Ed: B. Vernon), Woodhead Publishing, Cambridge, UK **2011**, Ch. 3.
[34] S. V. Murphy, A. Atala, *Nat. Biotechnol.* **2014**, *32*, 773.
[35] T. R. Hoare, D. S. Kohane, *Polymer* **2008**, *49*, 1993.
[36] J. P. Rodríguez, M. González, S. Ríos, V. Cambiazo, *J. Cell. Biochem.* **2004**, *93*, 721.
[37] a) B. D. Fairbanks, M. P. Schwartz, A. E. Halevi, C. R. Nuttelman, C. N. Bowman, K. S. Anseth, *Adv. Mater.* **2009**, *21*, 5005; b) K. M. Schultz, K. A. Kyburz, K. S. Anseth, *Proc. Natl. Acad. Sci. USA* **2015**, *112*, E3757.
[38] a) J. S. Miller, K. R. Stevens, M. T. Yang, B. M. Baker, D.-H. T. Nguyen, D. M. Cohen, E. Toro, A. A. Chen, P. A. Galie, X. Yu, R. Chaturvedi, S. N. Bhatia, C. S. Chen, *Nat. Mater.* **2012**, *11*, 768; b) C. Colosi, S. R. Shin, V. Manoharan, S. Massa, M. Costantini, A. Barbetta, M. R. Dokmeci, M. Dentini, A. Khademhosseini, *Adv. Mater.* **2016**, *28*, 677; c) M. P. Cuchiara, D. J. Gould, M. K. McHale, M. E. Dickinson, J. L. West, *Adv. Funct. Mater.* **2012**, *22*, 4511.
[39] a) G. Silva, C. Czeisler, K. Niece, E. Beniash, D. Harrington, J. Kessler, S. Stupp, *Science* **2004**, *303*, 1352; b) A. Banerjee, M. Arha, S. Choudhary, R. S. Ashton, S. R. Bhatia, D. V. Schaffer, R. S. Kane, *Biomaterials* **2009**, *30*, 4695; c) T. C. Lim, W. S. Toh, L.-S. Wang, M. Kurisawa, M. Spector, *Biomaterials* **2012**, *33*, 3446.
[40] L. Jongpaiboonkit, W. J. King, W. L. Murphy, *Tissue Eng., Part A* **2009**, *15*, 343.
[41] N. Huebsch, P. R. Arany, A. S. Mao, D. Shvartsman, O. A. Ali, S. A. Bencherif, J. Rivera-Feliciano, D. J. Mooney, *Nat. Mater.* **2010**, *9*, 518.
[42] S. T. Laughlin, J. M. Baskin, S. L. Amacher, C. R. Bertozzi, *Science* **2008**, *320*, 664.
[43] C. M. Madl, M. Mehta, G. N. Duda, S. C. Heilshorn, D. J. Mooney, *Biomacromolecules* **2014**, *15*, 445.
[44] L. Cai, C. B. Dinh, S. C. Heilshorn, *Biomater. Sci.* **2014**, *2*, 757.
[45] T. P. Richardson, M. C. Peters, A. B. Ennett, D. J. Mooney, *Nat. Biotechnol.* **2001**, *19*, 1029.
[46] M. Greenwood-Goodwin, E. S. Teasley, S. C. Heilshorn, *Biomater. Sci.* **2014**, *2*, 1627.
[47] Y. Brudno, R. M. Desai, B. J. Kwee, N. S. Joshi, M. Aizenberg, D. J. Mooney, *ChemMedChem* **2015**, *10*, 617.
[48] H. Babu, G. Cheung, H. Kettenmann, T. D. Palmer, G. Kempermann, *PLoS ONE* **2007**, *2*, e388.
[49] K. Saha, A. J. Keung, E. F. Irwin, Y. Li, L. Little, D. V. Schaffer, K. E. Healy, *Biophys. J.* **2008**, *95*, 4426.